Basic Nickel Carbonate: Part I. Microstructure and Phase Changes during Oxidation and Reduction Processes

M.A. RHAMDHANI, E. JAK, and P.C. HAYES

A significant industrial problem associated with the production of nickel from basic nickel carbonate has been identified. Fundamental studies of the change of phase, product surface, and internal microstructures taking place during oxidation and reduction processes at temperatures between 110 °C and 900 °C have been carried out. The various elemental reactions and fundamental phenomena that contribute to the change of the physical and chemical characteristics of the samples during the processes taking place in Ni metal production through gas/solid-reduction processes have been identified and thoroughly investigated. The following phenomena affecting the final-product microstructure were identified as follows: (1) chemical changes, *i.e.*, decomposition, reduction reactions, and oxidation reactions; (2) NiO and Ni recrystallization and grain growth; (3) NiO and Ni sintering and densification; and (4) agglomeration of the NiO and Ni particles.

DOI: 10.1007/s11663-007-9124-4

I. INTRODUCTION

THIS article describes a series of fundamental studies to identify the elemental reactions and phenomena taking place during oxidation and reduction processes used in production of solid Ni metal. A great deal of fundamental research has been undertaken on the factors influencing the gas/solid reduction processes; this includes thermal decomposition reactions and heterogeneous reactions involving gas/solid systems.[1–6] These studies have formed the basis for the use of these reactions in metallurgical and materials production on an industrial scale. The evolution of materials characteristics during these processes is complex, since a number of elemental reactions and fundamental phenomena occur simultaneously; these may include, but are not limited to, solid-precursor decomposition, reduction reactions, oxidation reactions, gas- and solid-phase mass transfer, and sintering. Identifying and describing these fundamental phenomena is important for understanding the underlying science, as well as for improved control of technological applications. Differences in the relative contributions of these phenomena will lead to differences in the properties of the final product.

Despite the accumulated knowledge to date, the complexities of the processes mean that it is still necessary to characterize individual systems through systematic experimental studies. An important industrial example of the class of gas/solid-reaction processes is the production of nickel. Basic nickel carbonates ($NiCO_3{\cdot}xH_2O$, $NiCO_3{\cdot}xNi(OH)_2{\cdot}yH_2O$, $NiCO_3{\cdot}xNiO{\cdot}yH_2O$), or BNC, are used in the commercial production of nickel-metal powders and compacts through calcination and reduction with hydrogen.[7]

In the case of nickel production from nickel oxide, residual oxygen and overall reduction rate are the key parameters determining the specification and value of the final Ni product and the production rates, respectively. The European Union's new chemical policy regulations[8] require that oxygen concentrations in the nickel product are less than 0.1 wt pct as nickel oxide. These restrictions are driven by the need to minimise the generation of residual NiO dust, which has been shown to be carcinogenic.[9] From the point of view of workplace health and safety, and marketability of nickel products, it is important to characterize the form of any residual nickel oxides present, and to determine how they were formed, and therefore, how they might be further reduced. These processes, as they relate to industrial practice, have not been adequately described in studies to date.

The approach taken in the current study is as follows: (1) systematically investigate the modes of occurrences of residual oxygen (in the form of NiO) in the final Ni product; (2) carry out carefully planned and controlled laboratory experiments to investigate fundamental phenomena and reactions; and (3) relate results from these experiments to microstructures observed in industrial samples to identify fundamental processes occurring during production of Ni metal through gas/solid reactions.

Figure 1 illustrates the various types of residual NiO microstructures observed in materials obtained from several locations along the process line in the commercial production of Ni. For the purpose of the following

M.A. RHAMDHANI, formerly Postdoctoral Research Fellow, Pyrometallurgy Research Centre, School of Engineering, University of Queensland, is Lecturer, Faculty of Engineering and Industrial Sciences, Swinburne University of Technology, Hawthorn VIC 3122, Australia. E. JAK, Associate Professor, and P.C. HAYES, Professor, are with the Pyrometallurgy Research Centre, School of Engineering, University of Queensland, Brisbane QLD 4072, Australia. Contact e-mail: ARhamdhani@swin.edu.au

Manuscript submitted October 18, 2007.
Article published online February 14, 2008.

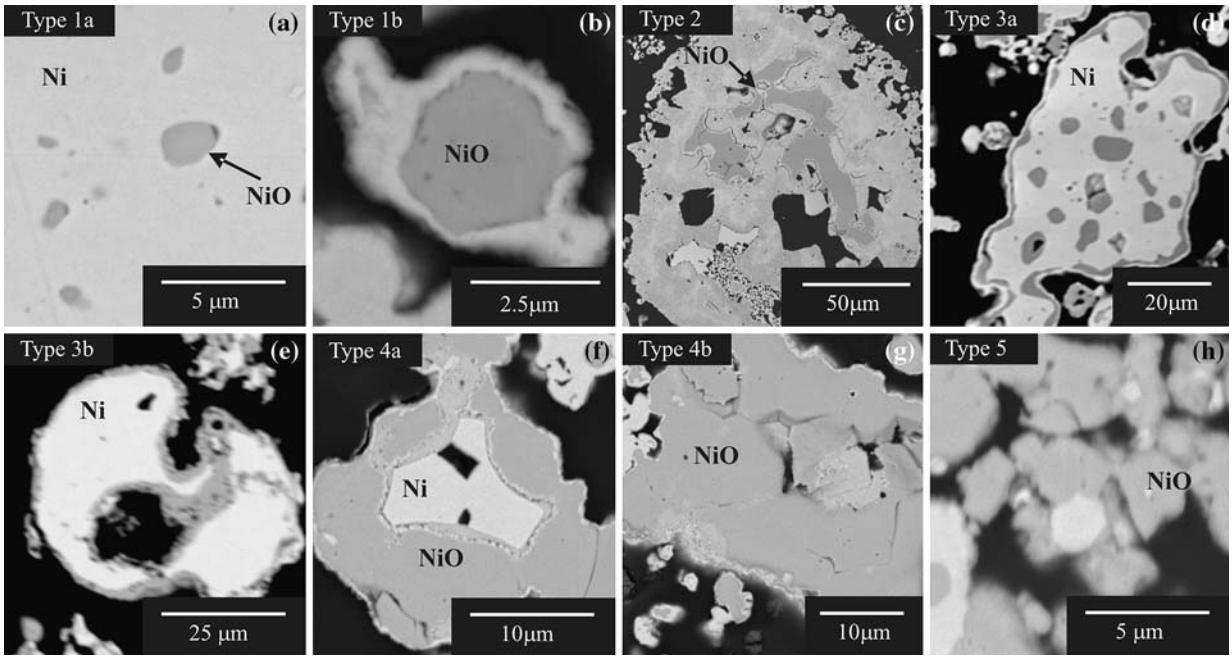

Fig. 1—Examples of types of residual nickel oxides observed in the materials and product of refinery plant: (*a*) type 1A, NiO enclosed by thick dense Ni; (*b*) type 1B, NiO enclosed by thin Ni layer; (*c*) type 2, trapped blocky NiO surrounded by porous Ni; (*d*) type 3A, NiO with fine layer of Ni on NiO surface; (*e*) type 3B, NiO on the surface of Ni; (*f*) type 4A, bulky NiO with dense Ni inside; (*g*) type 4B, bulky NiO; and (*h*) type 5, fine partially reduced NiO particles, size 1 to 5 μm.

systematic investigation of the processes resulting in formation of these various types of NiO, these have been classified as follows:

(1) type 1—trapped round particles surrounded by (1A) thick or (1B) thin dense Ni;
(2) type 2—trapped blocky form surrounded by porous Ni;
(3) type 3—surface layer of a NiO on a Ni particle (3A) with or (3B) without a fine layer of Ni on oxide surface;
(4) type 4—bulky NiO (4A) with or (4B) without dense Ni inside; and
(5) type 5—fine partially reduced NiO particles with individual particle size of one to five μm.

From Figure 1, it clearly follows that residual NiO is present in various complex structures, which resulted from different phenomena occurring during the Ni production process. Understanding of the phenomena resulting in the formation of these residual, nickel-oxide microstructures is important for the process control to obtain a high-quality nickel product.

In Part I of the series, a systematic investigation of changes in phases present, product surface, and internal microstructures occurring in starting material BNC during controlled oxidation and reduction conditions is provided. The principal aim of the study is to identify the various fundamental phenomena occurring and their effects on the processes and the final product. This is to provide a basis for future fundamental studies on each of the phenomena and also provide information in support of industrial operations. In Part II of the series, the analysis of the microstructure formation in intermediate and final products during industrial operations and the implications for plant practices are described.

II. PREVIOUS STUDIES ON BNC DECOMPOSITION AND NiO REDUCTION

There have been a number of studies on the thermal decomposition of BNC and nickel carbonates using thermo-gravimetric analysis (TGA) and differential thermal analysis (DTA).[10–14] It is generally agreed that the thermal decomposition of various BNC proceeds in two steps, first involving the removal of H_2O only, and then H_2O and CO_2. Using heating rates between 2 °C/min to 50 °C/min the evolution of H_2O only is reported to occur from 90 °C to 200 °C; the evolution of H_2O and CO_2 occurs from 270 °C to 420 °C. The two steps of decomposition of BNC can be represented by the following chemical reactions:

$$x\mathrm{NiCO_3}\cdot y\mathrm{Ni(OH)_2}\cdot z\mathrm{H_2O} \rightarrow x\mathrm{NiCO_3}\cdot y\mathrm{Ni(OH)_2} + z\mathrm{H_2O} \quad [1]$$

$$x\mathrm{NiCO_3}\cdot y\mathrm{Ni(OH)_2} \rightarrow (x+y)\mathrm{NiO} + x\mathrm{CO_2} + y\mathrm{H_2O} \quad [2]$$

The two decomposition steps are reported to apply to $2\mathrm{NiCO_3}\cdot 3\mathrm{Ni(OH)_2}\cdot 4\mathrm{H_2O}$,[11,13] $\mathrm{NiCO_3}\cdot 2\mathrm{Ni(OH)_2}\cdot 4\mathrm{H_2O}$,[12] and $\mathrm{NiCO_3}\cdot \mathrm{Ni(OH)_2}\cdot 2\mathrm{H_2O}$.[14] Only in the latter study[14] have the microstructure changes occurring during the transformation from BNC to NiO particles been

examined; however, this is a very cursory study of these phenomena.

There have been a number of studies on the gaseous reduction of nickel oxide to nickel by hydrogen-based gases,[15–21] in which the overall reaction can be expressed as follows:

$$NiO_{(s)} + H_{2(g)} \rightarrow Ni_{(s)} + H_2O_{(g)} \quad [3]$$

In many cases, the starting point for these studies involved the use of finely divided NiO powder or compacts. Although reduction in hydrogen atmospheres was found by many investigators to occur readily, there are considerable differences in the reported kinetics of these processes due to the differing characteristics of the starting materials and the reaction geometries employed in these studies.[15–21] In relatively few studies, the reaction conditions have been well established, using either dense NiO sheets[16–18] or granules[20,21] to overcome gas-phase mass-transfer limitations. These studies show that the reaction rates increase with increasing temperatures up to 600 °C, and then a slowdown between 600 °C to 900 °C, before increasing again above 950 °C. There are no phase changes taking place in this range of temperatures, and no physical changes to the oxide or metallic phases were detected that might explain the slowdown of the reaction between 600 °C to 900 °C. A number of mechanisms have been proposed to explain the observed reduction behavior, but to date, the origins of these phenomena remain uncertain.

The majority of the studies on BNC are focused on the thermal decomposition in air and limited to low temperatures (< 600 °C). On the other hand, although research has been carried out on NiO reduction at temperature ranges between 200 °C to 1000 °C, there are no published studies of microstructure evolution during reduction of BNC to NiO, and then to Ni.

Although the gaseous transformation of BNC to NiO, and then reduction to nickel by hydrogen appear to be simple reactions, the factors influencing the extent and rates of reduction, and its inter-relationship with the microstructure are not completely understood. The reduction of BNC and NiO appear to be strongly dependent on the characteristics of the starting materials, the process conditions, and thermal history. This is of particular concern for the accurate control of industrial processes used in the production of nickel oxide and nickel metal powders, in which variations in product quality and characteristics are undesirable.

III. EXPERIMENTAL DESIGN

A. *Materials*

In the current study, BNC supplied by the BHP Billiton Yabulu Refinery was used as the starting material. The BNC was produced by precipitation of nickel from an ammonia-ammonium carbonate solution. The particles were spherical and ellipsoidal in shape, as shown in Figure 2, ranging from 0.4 to 23 μm in diameter, with a mean diameter of 8.2 μm. The surfaces of the particles were superficially smooth; the Brunauer-Emmett-Teller (BET)-specific surface area of the original BNC particles was 238 m^2/g. Prior to experiments, BNC samples were dried in an oven in air atmosphere at a temperature of 105 °C for 16 hours to release the physically bound H_2O. The dried BNC contained approximately 52 pct wt Ni, 3.52 pct wt C, and approximately 0.001 pct wt S; the balance was predominantly O and H_2O. On this basis, the calculated composition is approximately $NiCO_3 \cdot 2.02Ni(OH)_2 \cdot 1.94H_2O$.

B. *Experimental Plan*

The experimental plan in the current study was developed following careful evaluation of the modes of occurrences of residual nickel oxide in the materials (Figure 1), the thermal and atmosphere conditions in the actual process, and consideration of possible elementary reactions and phenomena involved in the gas/solid reaction processes.

Separate and combination heat treatments on BNC samples under specific experimental conditions were

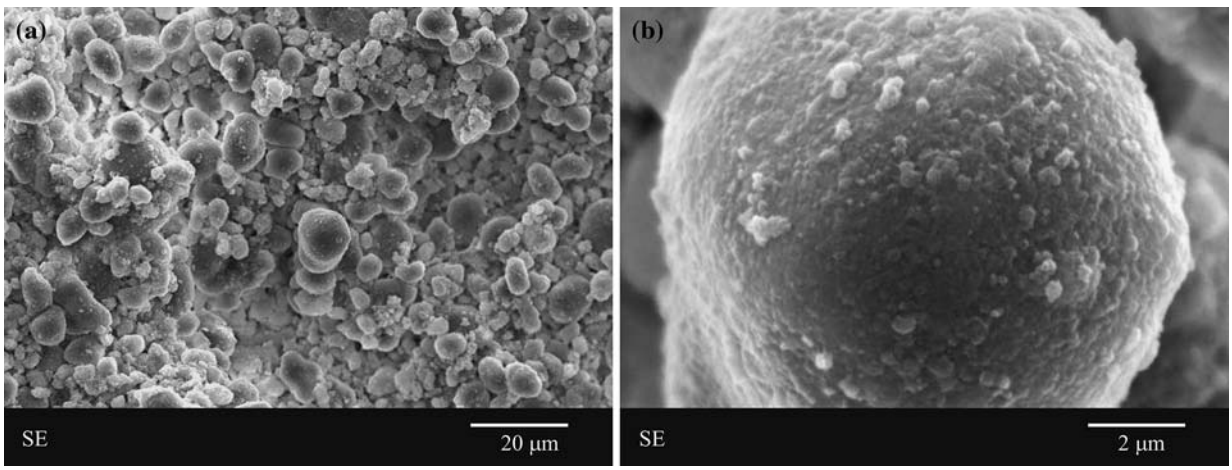

Fig. 2—SEM micrographs (secondary electron images) showing the surface morphology of the original BNC particles. Note the smooth surface of the particles, which consist of submicron grains.

carried out to reproduce some of the residual nickel-oxide microstructures to allow the investigation of the underlying elementary reactions and fundamental phenomena occurring during the process responsible for the formation of these microstructures.

The heat treatments carried out in this study are as follows: (1) calcination/oxidation of BNC in air; (2) direct reduction of BNC in reducing (15 pct H_2-N_2 and 1.5 pct H_2-N_2) gas atmosphere; and (3) reduction in 15 pct H_2-N_2 gas atmosphere of preoxidized/calcined BNC.

The calcination/oxidation and reduction of the samples were carried out at temperatures between 110 °C and 900 °C. The samples were held at the peak temperatures for 30, 60, and 120 minutes to evaluate the effect of holding time at a temperature. The heating rate of 10 °C/min used in the study was selected to reflect the heating rate in the rotary kiln used in industrial production of nickel.[22]

C. *Experimental Technique*

The oxidations and reductions were carried out in an electrically heated furnace inside a quartz tube, using a top-blown fluidising particle technique. The schematic of the furnace used in the current study is shown in Figure 3. The reducing/oxidizing gases were introduced through a 5-mm-inner diameter (ID) alumina injection tube from the top, blowing and circulating the particles at the bottom of the closed-end, 30-mm-diameter quartz tube. The flow rates utilized in the experiments were 500 to 1000 mL/min. The quartz tube was supported by a steel frame separate from the furnace, and it was moveable. A mechanical vibrator was attached to the steel frame, thus indirectly vibrating the quartz tube; this ensured that a good circulation of the particles in the sample bed was maintained throughout the experiments and enhanced the contact between the gas and the particles.

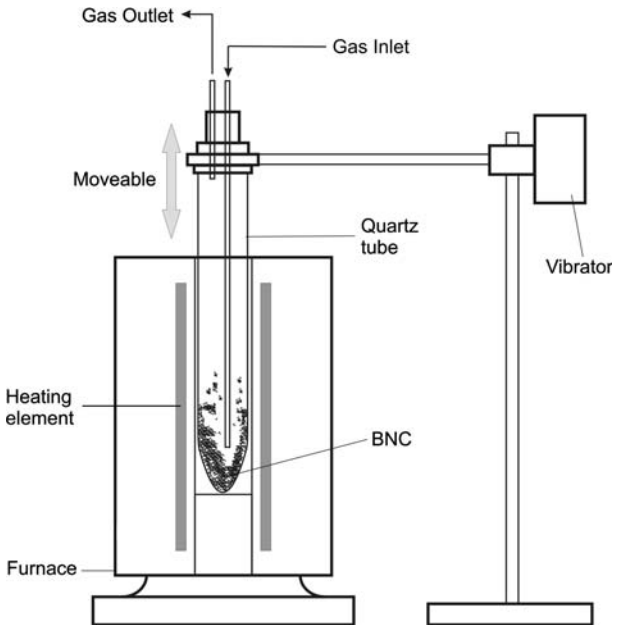

Fig. 3—Schematic of the experimental apparatus used to treat BNC powders.

Approximately 5 g of sample were initially placed in the quartz tube. The samples were heated to the desired temperature in the desired atmosphere. After reaching the desired temperature, the samples were held at the temperature before they were quickly cooled by removing the quartz tube from the furnace and by passing a flow of inert gas (Ar or N_2) through the system. The samples were then analyzed using materials-characterization techniques to study the phase changes and microstructure/surface-morphology evolution during the process. Selected repeated experiments were carried out to ensure the consistency and repeatability of the experiments.

D. *Analysis Techniques and Sample Preparation*

The microstructures of the samples were examined using scanning electron microscopy (SEM) and energy dispersive X-ray (EDX) techniques, namely, FE-SEM JEOL* 6300/6400, variable pressure SEM JEOL 6460LA, and PHILIPS** XL-30 with accelerating voltage of 15 and 20 kV. X-ray powder diffraction (XRD) analyses were carried out using PHILIPS PW 1130 X-ray diffractometer with a graphite monochromator using Cu K_α radiation.

*JEOL is a trademark of Japan Electron Optics Ltd., Tokyo.

**PHILIPS is a trademark of FEI Company, Hillsboro, OR.

Thermo-gravimetric analysis and DTA were carried out on the samples using the STA 409C/CD (NETZSCH GmbH, Bayern, Germany). Specific surface-area measurement of selected samples was carried out using the Tristar 3000 (Micromeritics Instrument Corp., Norcross, GA). Particle-size measurement of the samples was carried out using the Mastersizer 2000 (Malvern Instruments Ltd., Worchestershire, United Kingdom).

To enable the examination of the internal microstructures of the materials, the samples, after the experiments, were mounted in epoxy resin and cured in a vacuum chamber. Cross sections of the samples were then prepared by polishing, using SiC paper and diamond paste (down to a 0.25 μm size). For SEM surface-morphology observations, the powder samples after the experiments were directly placed on a carbon tab attached to an aluminium pin stub before being sputter coated using an Eiko IB-5 Sputter Coater (Eiko Co. Ltd., Hitachinaka, Japan) with platinum.

IV. RESULTS AND DISCUSSION

A. *BNC Samples Calcined in Air*

The behavior, fundamental reactions, and microstructural changes of BNC during calcination in air were

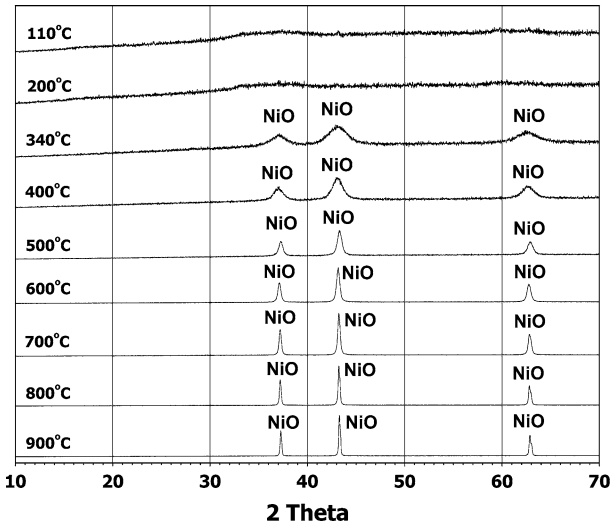

Fig. 4—XRD spectra of BNC samples calcined in air at various temperatures. Heating rate 10 °C/min, holding time at temperature 30 min, Cu K_α radiation used.

characterized using a number of techniques. Figure 4 shows the XRD patterns of BNC samples calcined in air for 30 minutes at various temperatures. The XRD analyses of the samples heated at 110 °C and 200 °C show no clear X-ray diffraction peaks, suggesting that the material was in an amorphous or microcrystalline state. At 340 °C, it can be seen that the NiO diffraction peaks appear, indicating that the reaction in Figure 2 had already commenced. As the temperature of calcination is increased to 900 °C, the NiO peaks become sharper.

From the XRD results, the average crystallite size of the NiO was estimated by using the Debye-Scherrer formula,[23] *i.e.*, calculated from the broadening of the X-ray peaks at half maximum, as follows:

$$D = 0.89\lambda/\beta\cos\theta \qquad [4]$$

where D is the average crystallite size, λ is the Cu K_α wavelength (1.5418 Å), and β is the peak width at half maximum. Assuming a zero contribution from strain, the values of β were corrected by considering the broadening due to instrumental effects.[23] The instrumental effects to the X-ray peaks broadening were determined by analysing NIST 640 C silicon standard and were found to have a value of $\beta_{inst} = 0.134$ deg. Table I shows the summary of the effect of maximum calcination temperature in air on the average NiO crystallite size. At 340 °C, the average crystallite size

Table I. Effect of Maximum Calcination Temperature in Air on the Average NiO Crystallite Size, Calculated Using Debye–Scherrer Formula (BNC Heating Rate 10 °C/min; Holding Time at Temperature 30 Minutes)

Temperature of calcination (°C)	340	400	500	600	700	800	900
Average crystallite size, D (nm)	4	7	16	24	34	44	52

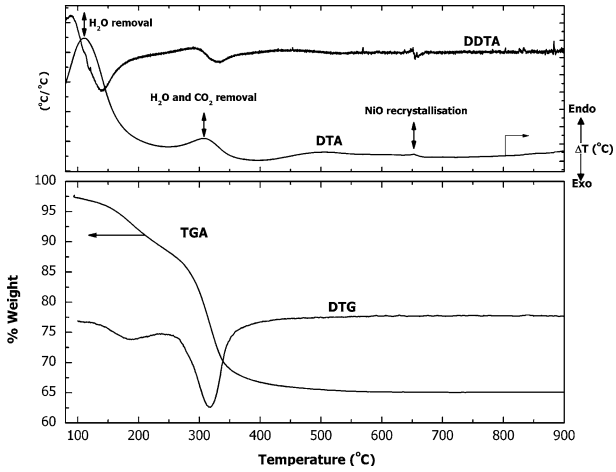

Fig. 5—DTA, TGA, DTG, and DDTA curves of BNC samples heated in air with heating rate of 10 °C/min.

was appromixately 4 nm; the average crystallite size increases with increasing calcination temperatures. At 900 °C, the calculated average crystallite size was approximately 52 nm (0.052 μm), and this value is comparable to the size of NiO grains observed using SEM, as demonstrated subsequently in this article.

Figure 5 shows the TGA and DTA results of BNC heated in air from room temperature to 900 °C, with a heating rate of 10 °C/min. The DTA curve shows two maxima at 110 °C and 310 °C, and the differential thermal gravimetry (DTG) curve suggests that the first decomposition of BNC occurred between 100 °C and 220 °C, and that the second decomposition occurred in the range of 230 °C to 370 °C. These may be attributed to the release of H_2O and the formation of nickel oxide (second removal of H_2O and CO_2), respectively, as has been suggested by previous investigators.[10–14] These observations and interpretations are supported by the XRD results that indicate that at 340 °C, nickel oxide had already formed.

Figures 6(a) through (h) represent selected SEM micrographs of the surface morphologies and the sectioned microstructures of BNC samples at various temperatures, following treatment in air. At 110 °C to 200 °C, the shapes and the sizes of the particles were still the same as in the original particles. Figures 6(a) and (b) show SEM images of the surface and internal microstructure of a BNC particle at 200 °C. In general, discrete particles were observed at that temperature, rather than agglomerates. In Figure 6(b), the particles appear uniform in cross section; however, on heating above 200 °C, a concentric layer structure can be seen in some of the particles.

The concentric layer structure became more distinct upon heating up to 400 °C and 600 °C (Figure 6(d)). Some of the larger particles consist of two or more concentric layer structure cores, indicating the successive formation of layers on the particles' surfaces during the precipitation reaction.

At 700 °C and 800 °C, there were signs that agglomeration had occurred during calcination; agglomerates in the range of 50 to more than 100 μm were observed at

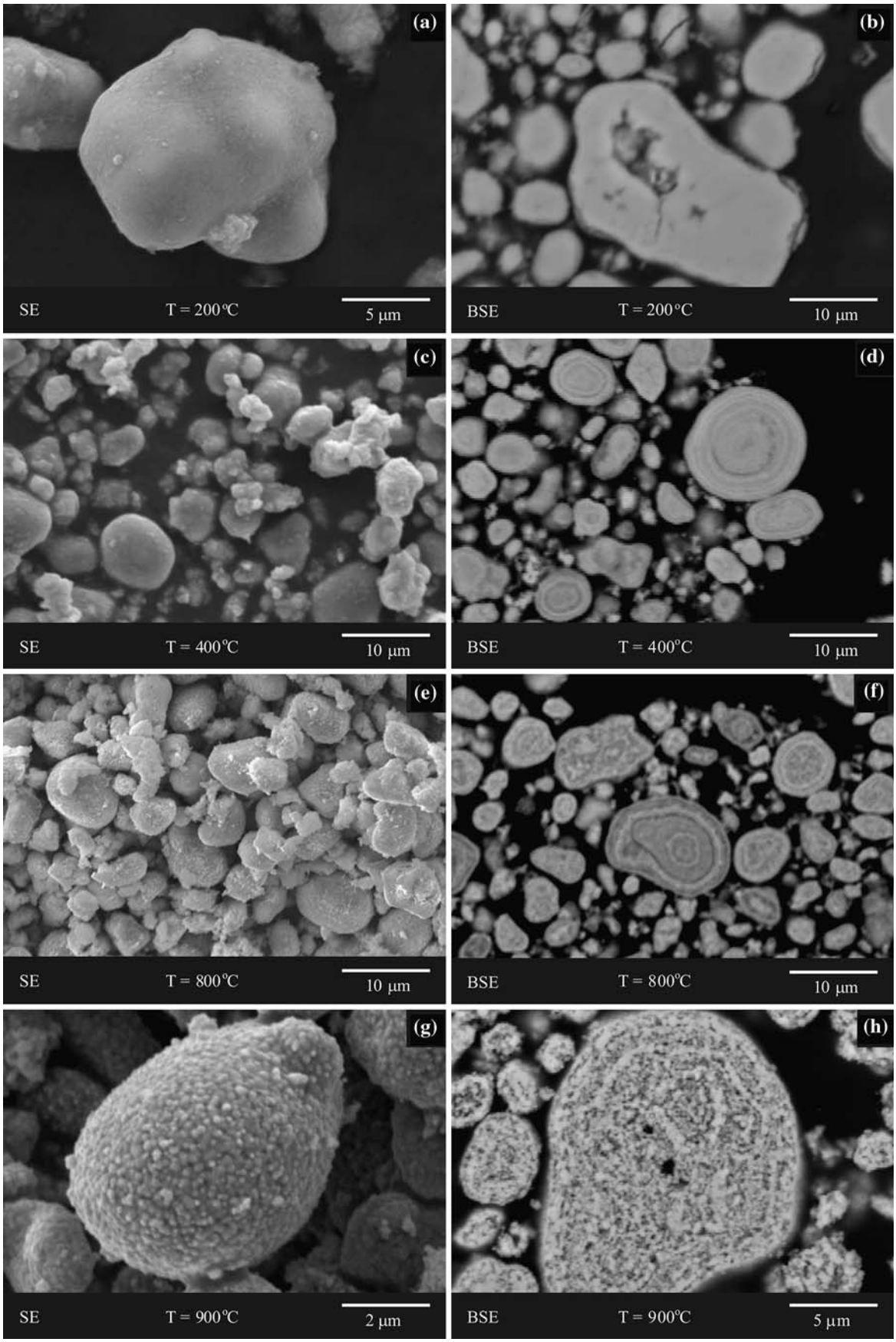

Fig. 6—SEM micrographs of the surface (left column) and the cross sections (right column) of BNC samples calcined in air (30 min, 10 °C/min heating rate) at various temperatures: (*a*) and (*b*) 200 °C; (*c*) and (*d*) 400 °C; (*e*) and (*f*) 800 °C; and (*g*) and (*h*) 900 °C.

800 °C. In some particles, a clear, physical separation between layers in the concentric layer structure had occurred by 800 °C. At temperatures in the range of 800 °C to 900 °C, random distributions of a very small (< 0.1 μm) recrystallized NiO grains were observed throughout the particles, destroying the concentric layer structure.

Referring to the results in Figure 5, it can be suggested from a small DTA peak at 660 °C that the recrystallization of NiO occurred at that temperature. This peak can be clearly seen in the first derivative of differential thermal analysis (DDTA) curve. The newly recrystallized NiO grains were, however, indistinguishable at 700 °C and 800 °C, which was likely due to the very small size of the grains. From the XRD peaks in Figure 4, the calculated average crystallite sizes at 700 °C and 800 °C were 34 and 44 nm, respectively. Figures 6(g) through (h) show SEM images of the surface and sectioned particles at 900 °C. It can be clearly seen from Figure 6(h) that submicron grains, having diameter of approximately 0.05 to 0.1 μm, are observed on the surface and within the particle. This is consistent with the average crystallite size calculated using the Debye–Scherrer formula (0.052 μm).

B. *BNC Sample Reduced in 15 Pct H_2-N_2 Gas Atmosphere*

To study the behavior, fundamental reactions and microstructure change of BNC in reducing conditions, BNC samples were again heated to various temperatures using a 10 °C/min heating rate, but in this series of experiments, a 15 pct H_2-N_2 gas atmosphere was used.

Figure 7 shows the XRD analyses of the samples reduced in 15 pct H_2-N_2 at different temperatures. It can be seen that at 100 °C to 200 °C, no peaks are observed, indicating the samples were in an X-ray amorphous state. At 340 °C, broad NiO X-ray diffraction peaks

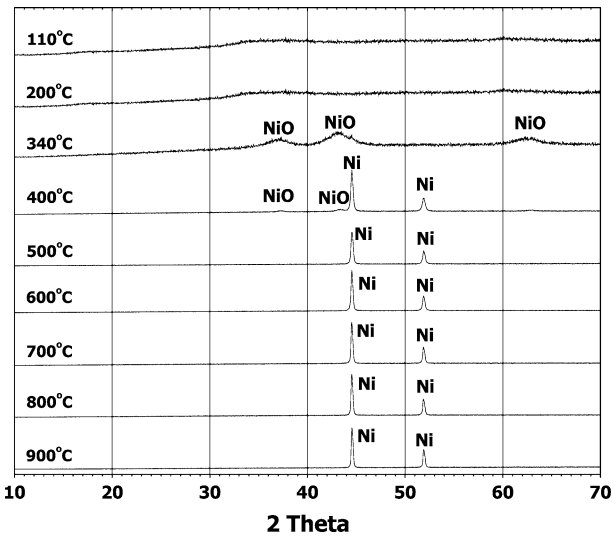

Fig. 7—XRD spectra of BNC sample reduced in 15 pct H_2-N_2 at various temperatures. Heating rate 10 °C/min, holding time at temperature 30 minutes, Cu K_α radiation used.

are observed, which indicate the formation of a fine-crystalline oxide. A small Ni-metal peak is also observed at this temperature. These suggest that upon heating in a reducing atmosphere, BNC first decomposes to nickel oxide, before forming nickel nuclei. At 400 °C, the X-ray diffraction pattern consists principally of Ni with residual NiO. Upon increasing the temperature to 900 °C, the Ni X-ray diffraction peaks become sharper.

At 100 °C to 200 °C, the surface morphology of the particles was similar to BNC particles oxidized at 110 °C to 200 °C in air. The majority of the 1- to 10-μm particles were spherical or ellipsoidal in shape, having smooth external surfaces. The sectioned microstructure of BNC particles at 200 °C appeared to be uniform, with concentric layer structure observed in some of the particles.

Figures 8(a) and (b) show SEM images of the surface and microstructure of sectioned particles at 340 °C. From the cross-sectional observation, it can be seen that at this temperature, some of the particles had transformed to more porous/spongy particles (Ni particles). The concentric layer structure of the particles at this temperature was quite distinct. Agglomeration of some of the Ni particles was observed at 340 °C.

The SEM observations of the particles treated at 400 °C to 500 °C showed that the surfaces of most particles were covered with porous/spongy Ni and that extensive agglomeration of the particles had occurred. The size of the agglomerates can be more than 100 μm. By 500 °C, it appears that all of the particles had transformed to porous Ni crystals, confirming the XRD results.

At 700 °C, the spongy nickel particles consisted of 0.05- to 0.1-μm-diameter nickel grains (Figures 8(c) and (d). At 800 °C, grain growth of the subgrains had occurred, such that the mean grain size of the nickel was of the order 1 μm. Extensive agglomeration of the particles at 800 °C can be seen in Figures 8(e) and (f).

At 900 °C, the particles had formed agglomerates/lumps of more than 700 μm in diameter. The Ni grains had coarsened to more than 1 μm in size. There was clear evidence of sintering and densification of the Ni structure (Figures 8(g) and (h)). From the particle cross sections, there was no evidence of residual nickel-oxide trapped inside the dense nickel; the darker regions at the center of the particles in Figure 8(h) are isolated pores.

Additional experiments were carried out using longer reduction times at the peak temperatures, *i.e.*, 60 and 120 minutes. Above 700 °C, there was a significant sintering/densification of the nickel when the reduction time was increased to 60 or 120 minutes (Figure 9).

The X-ray powder diffraction results and SEM observation were related to the DTA and TGA results. Figure 10 is an example of the DTA and TGA results; in this case, the reduction of BNC was carried out in 5 pct H_2-N_2 (rather than in 15 pct H_2-N_2) with a heating rate of 10 °C/min. This atmosphere condition was selected after considering the constraint of the instrument in using high hydrogen content gases and the safety assessment associated with the experimental procedure. However, it was expected that this would resemble the case of reduction in 15 pct H_2-N_2. From the DTA and DTG curves, it could

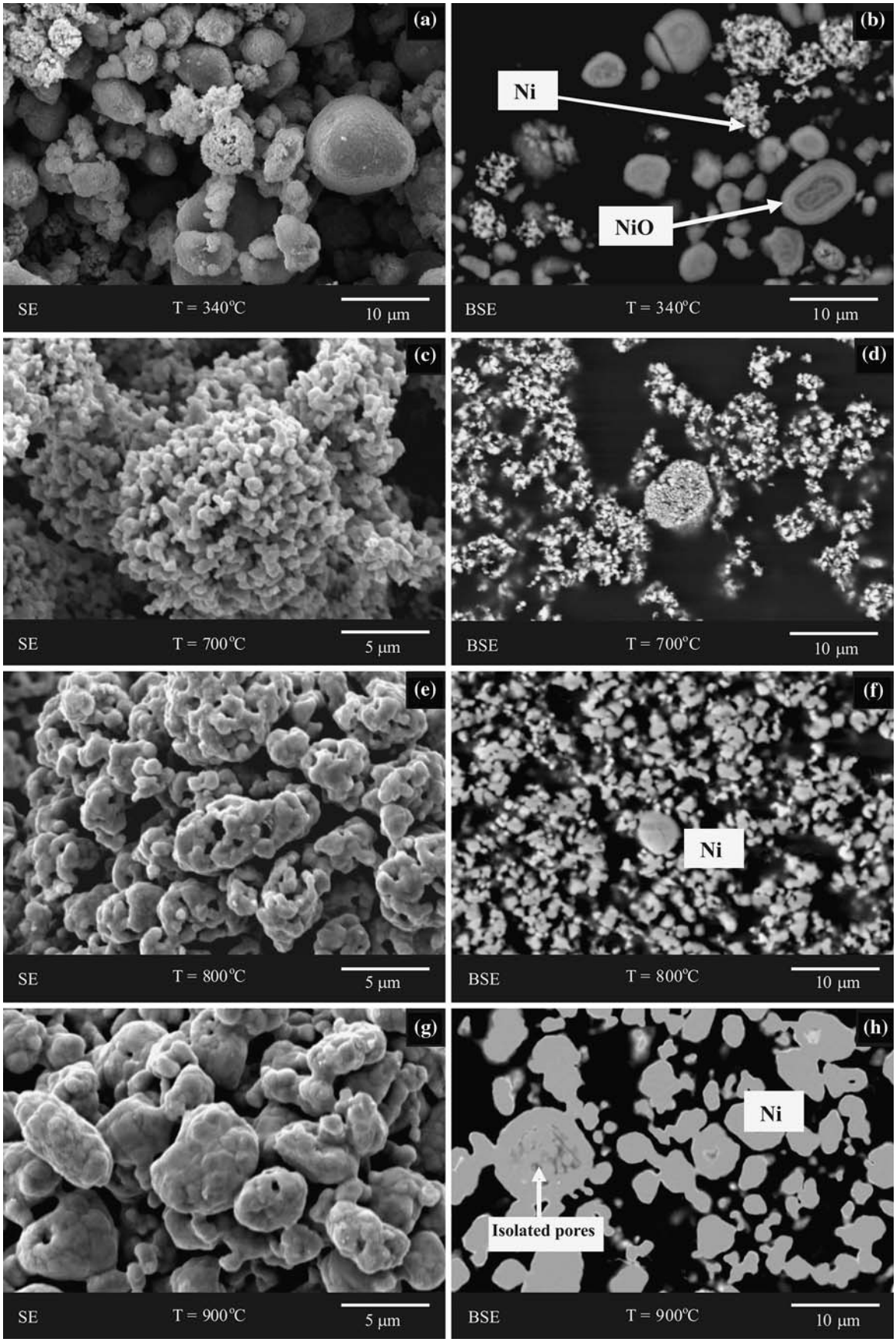

Fig. 8—SEM micrographs of the surface (left column) and the sections (right column) of BNC sample reduced in 15 pct H_2-N_2 (30 min, 10 °C/min heating rate) at various temperatures: (*a*) and (*b*) 340 °C, (*c*) and (*d*) 700 °C, (*e*) and (*f*) 800 °C, and (*g*) and (*h*) 900 °C. Nickel metal appears as the bright phase in (b).

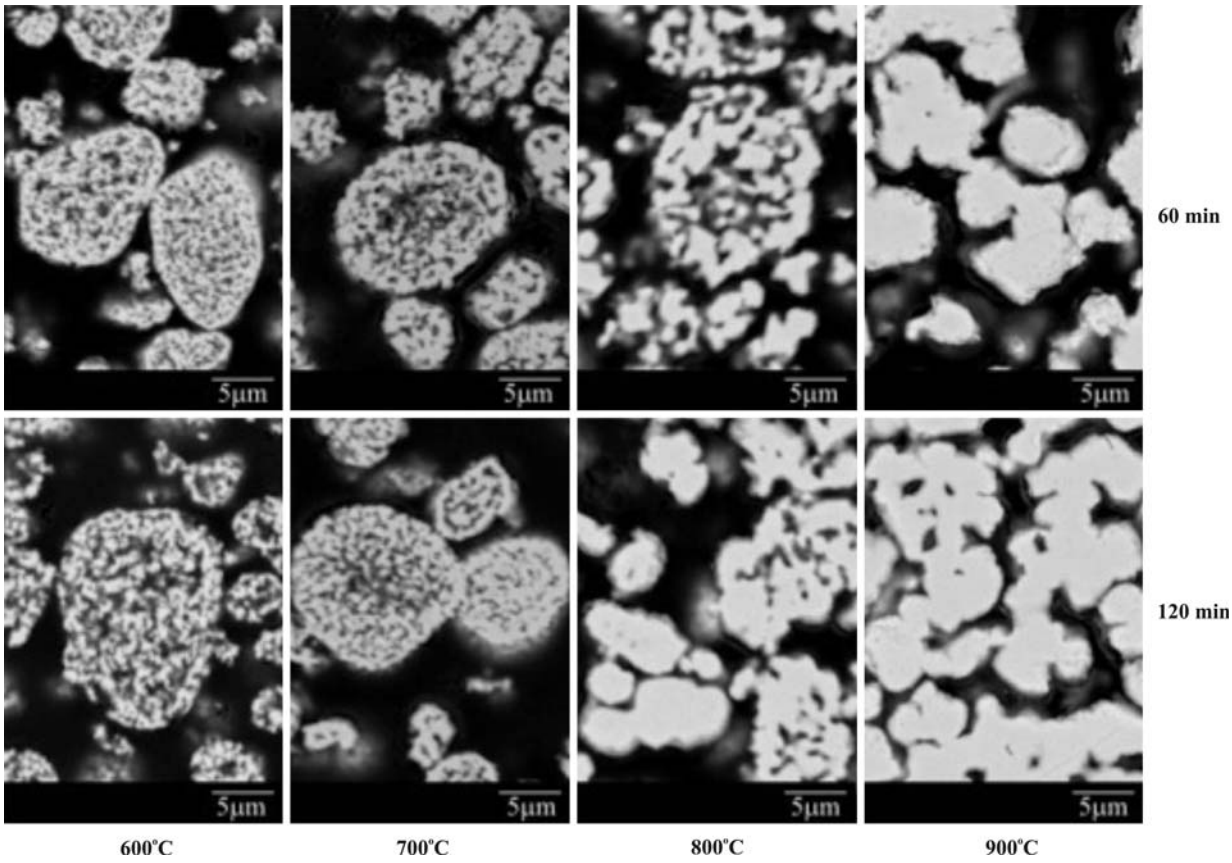

Fig. 9—SEM micrographs of the cross sections of BNC samples reduced in 15 pct H_2-N_2 at 60 and 120 min (10 °C/min heating rate) at various temperatures, showing extensive densification at temperatures above 700 °C.

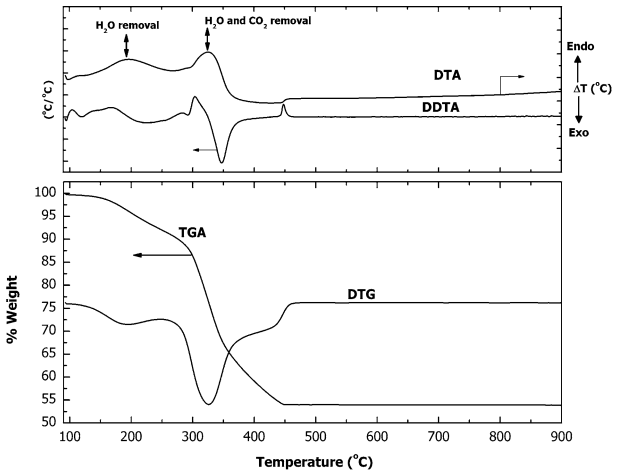

Fig. 10—DTA, TGA, DTG, and DDTA curves of BNC samples reduced in 5 pct H_2-N_2 with a heating rate of 10 °C/min.

be suggested that the decomposition of BNC to NiO occurred from 80 °C to approximately 370 °C, followed by NiO reduction to Ni occurring at approximately 450 °C. Absence of thermal and weight changes recorded by DTA and TGA curves indicates that no reactions occurred at temperatures above 500 °C; this is in agreement with microstructural and XRD analyses that indicate nearly complete reduction to Ni metal. The recrystallization and densification of Ni at temperatures higher than 700 °C, as evident from SEM observations, are not detected in the DTA spectrum, which may be due to the associated energy changes being very small.

C. *Preoxidized BNC Sample Reduced in 15 Pct H_2-N_2 Gas Atmosphere*

During the BNC processing, for example, in a rotary kiln, the material moves from low-temperature oxidizing conditions at the feed input end to high-temperature reducing conditions at the discharge end. In order to simulate this, and to study the effect of preoxidation on the reduction behavior, BNC samples were first preoxidized in air, with a 10 °C/min heating rate to 900 °C, then reduced in a 15 pct H_2-N_2 gas atmosphere at various fixed temperatures for 30 minutes.

Figure 11 shows the XRD analyses of the preoxidized BNC samples reduced at different temperatures. At 110 °C to 200 °C, the reduction was not started. Similarly to the directly reduced BNC, nickel started to nucleate at the temperature range of 300 °C to 400 °C. This is suggested from the XRD spectra at 340 °C and 400 °C showing Ni peaks. At 500 °C to 600 °C, from the XRD result, it can be seen that the height of the highest Ni peak is comparable to the highest NiO peak. In contrast to the directly reduced BNC, residual NiO was detected by XRD even at

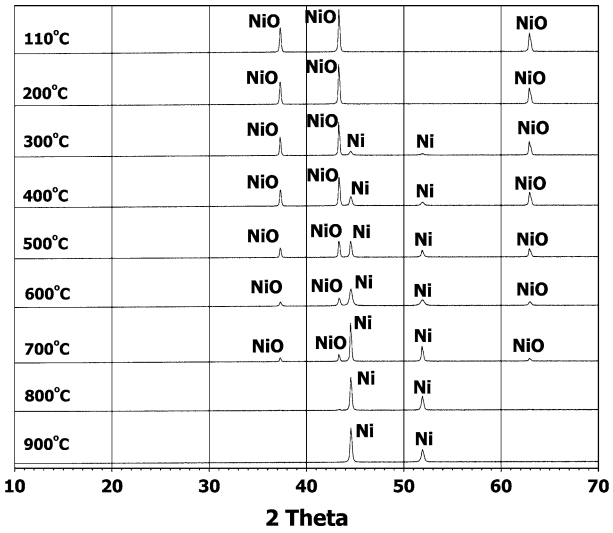

Fig. 11—XRD spectra of the preoxidized BNC samples in air at 900 °C (30 min, 10 °C/min heating rate), which were then reduced in 15 pct H_2-N_2 (30 min, 10 °C/min heating rate) at various fixed temperatures; Cu K_α radiation is used.

700 °C. At 900 °C, no NiO XRD peaks were observed; however, microstructure observation revealed the presence of residual NiO (Figure 12).

The morphology and microstructure of the particles after heating in 15 pct H_2-N_2 between 110 °C and 200 °C are similar to that of the starting preoxidized particles. The particles exhibited a structure that is composed of a random distribution of a very small (< 0.1 μm) recrystallized nickel-oxide grains, rather than a clearly defined layer structure.

Figures 12(a) and (b) show the morphology of the surface and microstructure of sectioned particles at 340 °C. In this temperature range, the particles started to agglomerate as the nickel formed at the surface, provides bridges between particles. The size of the agglomerates can be more than 400 μm.

Between 500 °C to 600 °C, surface pores were observed on the nickel particles; the size can be up to 1 μm or more (Figure 12(c)). A concentric layer structure with distinct gaps between layers was observed in some of the particles (Figure 12(d)).

At 700 °C, quite dramatic changes in the nickel-product structure were initiated with the densification of the nickel metal on the surface of the particles, resulting in the formation of a dense, nickel layer on the particle surface (Figures 12(e) and (f)).

At 800 °C and 900 °C, the particles were characterized by the presence of thick, dense, metallic-Ni layer that encapsulates the residual NiO inside the particles (Figures 12(g) and (h)). This dense nickel consists of recrystallized nickel with large-grain size, and the particles were sintered together. The thick, dense Ni made further reduction of the NiO by direct access of H_2 gas impossible.

Figure 13 is an example of the DTA and TGA results of the reduction in 5 pct H_2-N_2 (heating rate of 10 °C/min) of preoxidized BNC in air at 900 °C for 30 minutes. The decrease in weight starting at 340 °C, as can be seen from the TGA curve, suggests that NiO starts to reduce at approximately this temperature. This NiO reduction, however, continued up to 900 °C. This is in contrast with the direct reduction of BNC in the same atmosphere where the transformation to Ni is completed at 450 °C (Figure 10).

D. *Transformation Sequence*

The experimental results have shown that the microstructural changes taking place in the processing of BNC depend critically on the thermal history. The key changes in the samples during the experiments, derived by interpretation of results of the various analyses described previously, are summarized in Table II. The changes in the specific surface area, measured using the BET method, during BNC processing are summarized in Table III. The results of the specific surface-area measurements support the interpretation of transformations derived from SEM and other analyses.

In an oxidizing condition, *i.e.*, in air, BNC decomposition is believed to occur in two stages. The first stage involves the removal of physically absorbed water. The formation of NiO occurs at the second stage at a temperature between 300 °C to 400 °C; this transformation occurs without significant change in the specific surface area, *i.e.*, from 238 m^2/g in the original BNC to 204 m^2/g at 340 °C (Table III). At approximately 660 °C, the recrystallization of NiO commences; as the temperature increases, sintering and grain growth of the recrystallized NiO grains take place within the original particles. By 700 °C, these processes have resulted in a significant decrease of specific surface area to 6.6 m^2/g; at 900 °C, fully recrystallized NiO particles are formed with specific surface area of 1.1 m^2/g.

Direct gaseous reduction of BNC is suggested to take place in three stages. The first stage is the removal of physically entrained water. In the second stage, BNC decomposes to nickel oxide, accompanied by the removal of chemically bound H_2O and CO_2, producing particles having a porous, concentric-ring structure. In the third stage, nickel oxide is reduced to nickel metal, accompanied by the removal of oxygen. All of these changes can occur at relatively low temperatures, *i.e.*, below 500 °C.

Similar to the case of calcination in air, at these low temperatures, the NiO particles produced from the decomposition of BNC are porous (Figure 8(b)); as a consequence, they still have a high, specific surface area, *i.e.*, 207 m^2/g at 340 °C. This high, specific surface area facilitates the delivery of fresh reducing gas to the interior of the particles, thus promoting the complete reduction of the nickel oxide at low temperatures, provided it has a high, chemical rate of NiO reduction, *i.e.*, a high partial pressure of hydrogen (15 pct H_2-N_2). Further increases in temperature, *i.e.*, above 500 °C, result in the densification of the nickel product, accompanied by a significant decrease in specific surface area, *i.e.*, the specific surface areas at 700 °C and 900 °C are 1.1 and 0.3 m^2/g, respectively.

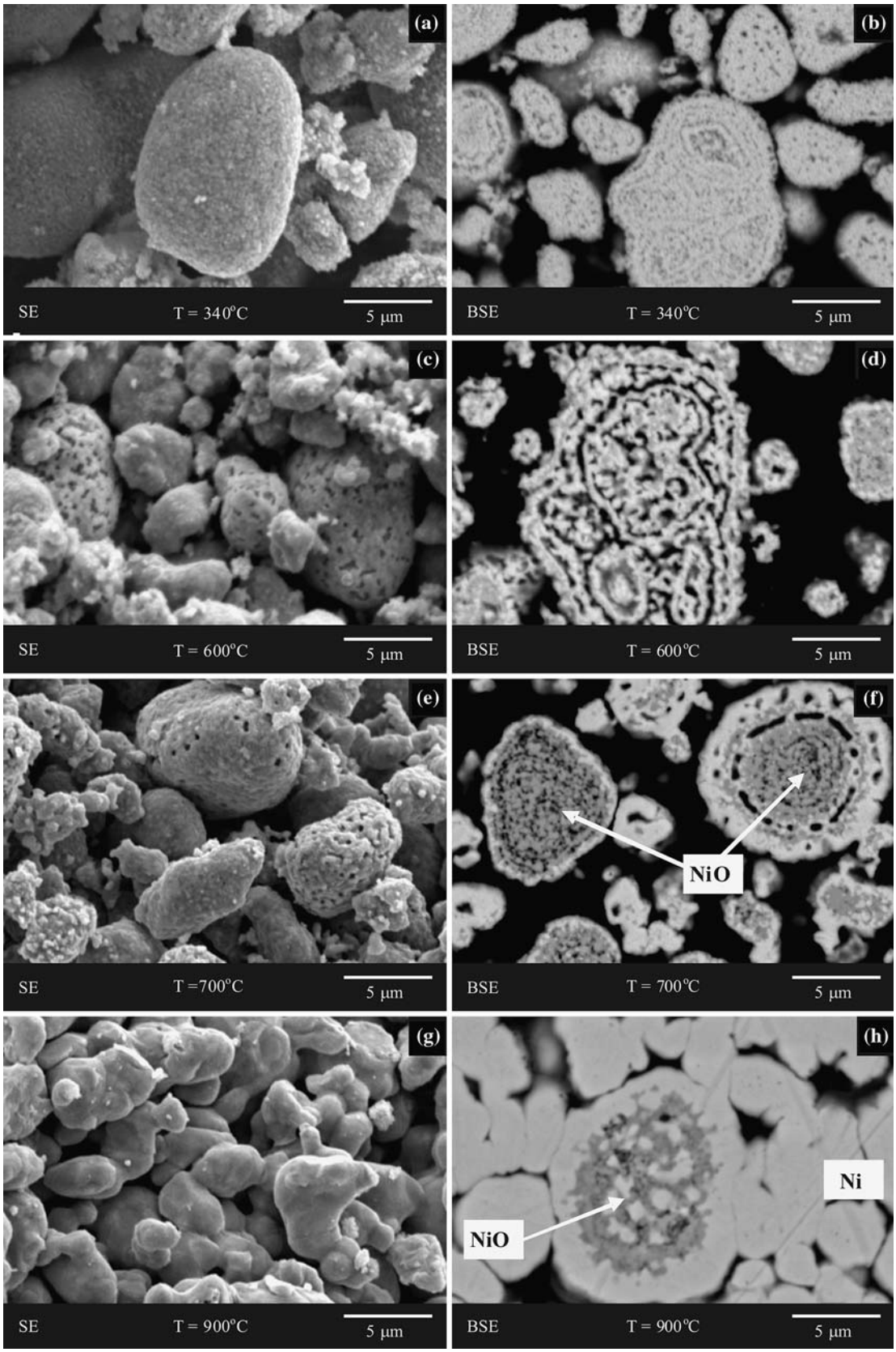

Fig. 12—SEM micrographs of the surface (left column) and the sections (right column) of the preoxidized (for 30 min at 900 °C, 10 °C/min heating rate) BNC sample reduced in 15 pct H_2-N_2 (30 min, 10 °C/min) at various temperatures: (*a*) and (*b*) 340 °C, (*c*) and (*d*) 600 °C, (*e*) and (*f*) 700 °C, and (*g*) and (*h*) 900 °C. (NiO and Ni appear as dark gray and bright phases, respectively, in (*d*), (*f*), and (*h*)).

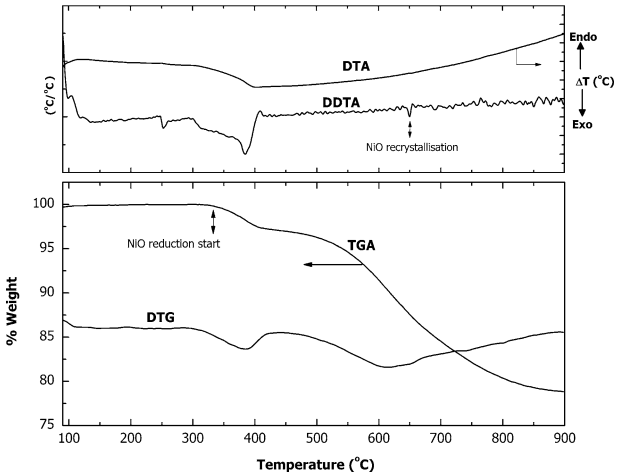

Fig. 13—Differential thermal analysis (DTA), thermal gravimetry analysis (TGA), first derivative of TGA (DTG), and first derivative of DTA (DDTA) curves of pre-oxidised BNC (at 900 °C, 30 min, with heating rate 10 °C/min) samples reduced in 5%H_2-N_2 with heating rate 10 °C/min.

In the case of the preoxidized BNC (at 900 °C) reduced in a 15 pct H_2-N_2 condition at 300 °C to 400 °C, the nickel metal nucleates on the surface of the recrystallized NiO grains. The reduction, however, proceeds at a slower rate compared to the directly reduced BNC. This is believed to be mainly due to the larger grain size, denser sintered structure, and higher crystallinity (low reducibility) of the recrystallized nickel oxide particles as a result of preoxidation. This observation is supported by the BET-specific surface-area measurements. Table III shows that the specific surface area of the preoxidized samples at 900 °C is 1.1 m^2/g.

As the temperature is increased to 660 °C, it appears that recrystallization of the unreduced NiO occurs, as could be suggested from the small peak in the DDTA curve in Figure 13. As the temperature reaches 700 °C to 800 °C, recrystallization, grain growth, and sintering of the nickel-metal product take place. As a result, there is a closing of pores on the particles' surfaces. Under the process conditions with the materials used in the current study, the rate of nickel densification (closing up of the pores) on the particle surface progresses quickly, relative to the overall reduction, resulting in the formation of a dense, nickel-metal product layer before the full reduction of the nickel oxide is complete. Once this dense, nickel microstructure has formed, further reduction of this trapped nickel oxide becomes progressively more difficult. There is no direct contact between the reducing gas and the nickel oxide at this stage; further removal of oxygen can only take place by solid-state diffusion through the dense, nickel layer formed, *i.e.*, the reaction becomes mass transfer limited. As further oxygen is removed in this way, the layer thickness of the dense nickel becomes progressively greater, and the diffusion flux of oxygen through the layer is progressively reduced. Prolonged heating times at high temperatures (> 800 °C) will also have a negative effect, as it promotes densification of overall agglomerated material. This is supported by the BET-specific, surface-area measurements; the specific surface area of the preoxidized (at 900 °C) samples reduced at 700 °C and 900 °C are 0.52 and 0.44 m^2/g, respectively.

This analysis indicates that the strategy to approach a more complete reduction of nickel oxide to nickel metal is to control the relative rate of densification of nickel product to the overall NiO reduction rate. To demonstrate this point, additional sets of experiments were carried out.

Initial tests were conducted by first oxidizing BNC at 500 °C for 30 minutes prior to subsequent isothermal reductions at 500 °C to 900 °C in 15 pct H_2-N_2 for 30 minutes. The temperature of 500 °C was chosen as the preoxidation temperature for the following reasons:

(1) at this temperature, the nickel oxide formed has lower crystallinity, higher porosity, and a higher surface/volume ratio, as compared to NiO preoxidized at 900 °C (Figure 4); and
(2) 500 °C is well below the Ni and NiO recrystallization temperatures of 600 °C to 700 °C (Table II) and below the temperature of 700 °C, at which the sintering and the densification of the porous nickel product is first observed (Table II).

The selected microstructures of BNC samples preoxidized at 500 °C, and subsequently reduced at 500 °C to 900 °C, are shown in Figures 14(a) through (d). From the microstructures, it can be seen that even at 500 °C, the nickel oxide has completely reduced to nickel metal. This result is in sharp contrast with samples preoxidized at 900 °C, then reduced at the same temperatures (Figure 12) for 30 minutes, in which NiO is trapped inside layers of dense, nickel metal. This demonstrates that controlling the nickel-oxide structure prior to reduction process, *i.e.*, increasing its reducibility, can result in a complete reduction of BNC to nickel. The key changes observed in the samples from this set of experiments are also summarized in Table II.

The second series of tests conducted was direct reduction of BNC in 1.5 pct H_2-N_2 at temperatures between 600 °C and 900 °C. Figure 15 shows selected SEM micrographs from these tests. It can be seen that at 700 °C, residual NiO trapped inside dense nickel was observed. This is not observed in the case of reduction in 15 pct H_2-N_2 at the same temperature. By decreasing the partial pressure of hydrogen by an order of magnitude, the chemical rate of reduction of nickel oxide is decreased; the densification of nickel product occurs before the reduction of nickel oxide is complete, which results in the formation of trapped residual nickel oxide. As the temperature is increased, more densification and agglomeration of the nickel occurs, which means further removal of the trapped NiO is more difficult. At 800 °C and at 900 °C, residual NiO enclosed in a dense Ni network, forming denser agglomerates, is observed (Figures 15(c) and (d)).

Previous studies of the reduction of NiO with hydrogen gas[10–16] have shown that reduction to metallic nickel occurs readily with the formation of porous, nickel metal product. The porous product allows continuous access by gas-phase diffusion from the bulk gas to the NiO interface, at which a chemical reaction

Table II. Summary of the Key Changes Observed during the Processing of BNC; Heating Rate 10 °C/min; Holding Time 30 Minutes

Temp. (°C)	BNC Calcined in Air	BNC Reduced in 15 Pct H_2-N_2	BNC Reduced in 1.5 Pct H_2-N_2	Preoxidized BNC (at 900 °C), Reduced in 15 Pct H_2-N_2	Preoxidized BNC (at 500 °C), Reduced in 15 Pct H_2-N_2
25 to 300	decomposition of amorphous BNC particles	decomposition of amorphous BNC particles	not investigated	fine grained (0.05 to 0.5 μm) NiO crystalline	not investigated
300 to 400	transformation from amorphous BNC (1 to 10 μm in diameter) to crystalline NiO	transformation of BNC to NiO; initial nucleation and growth of a porous Ni metal; some agglomeration of particles	not investigated	initial nucleation and growth of porous Ni metal product; some agglomeration of particles	not investigated
400 to 600	a concentric layered grain structure within each particle is formed; however, each particle remains physically intact	growth of porous Ni product; growth of Ni subgrains of 0.05 to 0.1 μm diameter	nucleation and growth of porous Ni; reduction of NiO is still occurring	reduction to Ni continues; agglomeration of particles	complete reduction of NiO forming porous multigrain Ni particles
600 to 800	recrystallization of NiO grains begins; sintering of NiO particles initiated	coarsening of Ni subgrains to 0.2 to 0.5 μm; evidence of sintering and agglomeration of Ni grains and particles	sintering and densification of Ni product on the surface of particles; evidence of NiO entrapped in thin dense Ni	substantial recrystallization of Ni subgrains and the formation of dense Ni layers on the surface of the particles; some residual NiO present inside particles	densification of porous nickel particles
800 to 900	formation of <0.1-μm-sized grains within the particles; further sintering and agglomeration of NiO	Subgrains form 0.5- to 2-μm dense grains, within fully recrystallized Ni particles; no evidence of NiO trapped inside Ni product	agglomeration of Ni particles; residual NiO remains, surrounded by thick dense recrystallized Ni	further agglomeration of dense Ni product grains; residual NiO remains in the interior of some of the particles surrounded by dense recrystallized Ni	more densification and agglomeration of Ni particles; no evidence of residual NiO in the interior of the particles

Table III. Summary of the Measured BET Specific Surface Areas from the Processing of BNC (Heating Rate 10 °C/min; Holding Time 30 Minutes)

	BET Specific Surface Area (m^2/g)		
Temperature (°C)	BNC Calcined in Air	BNC Reduced in 15 Pct H_2-N_2	Preoxidized BNC (at 900 °C), Reduced in 15 Pct H_2-N_2
25 (initial)	238	238	1.1
340	204	207	1.5
700	6.6	1.2	0.5
900	1.1	0.3	0.4

between gas and oxide occurs. The resultant H_2O product gas is also able to diffuse through the porous product, thus enabling the reduction reaction to proceed to completion. It has been shown in the present study that under certain conditions, the morphology of the Ni-metal product microstructure can change, leading to the change in the rate-limiting reaction mechanism. The formation of a dense, product layer leads to a significant reduction in the overall rate of oxygen removal from the sample.

Utigard *et al.*[20] reported that in temperature range of 700 °C to 900 °C, there is a decrease in the NiO reduction rates. Based on their extended experiments, they suggested that this is not due to physical changes of the oxide, nor the metallic phases. They speculated that the slowdown in the rate might be due to grain growth of the nickel formed or by surface segregation of sulfur. It should be noted that the characteristics, such as particle size, purity, *etc.*, of the NiO and experimental technique used in their study are different than that used in the current study.

The current study shows that in the temperature range of 700 °C to 900 °C, there are several fundamental phenomena occurring simultaneously that may be responsible for the lowering of the NiO reduction kinetics. These include the NiO recrystallization and grain growth (600 °C to 900 °C); NiO sintering (> 800 °C); Ni product recrystallization and grain growth (> 700 °C); Ni product densification (> 700 °C); and agglomeration of particles (> 700 °C). It is also shown in the present study that the thermal history and original microstructure of the material have

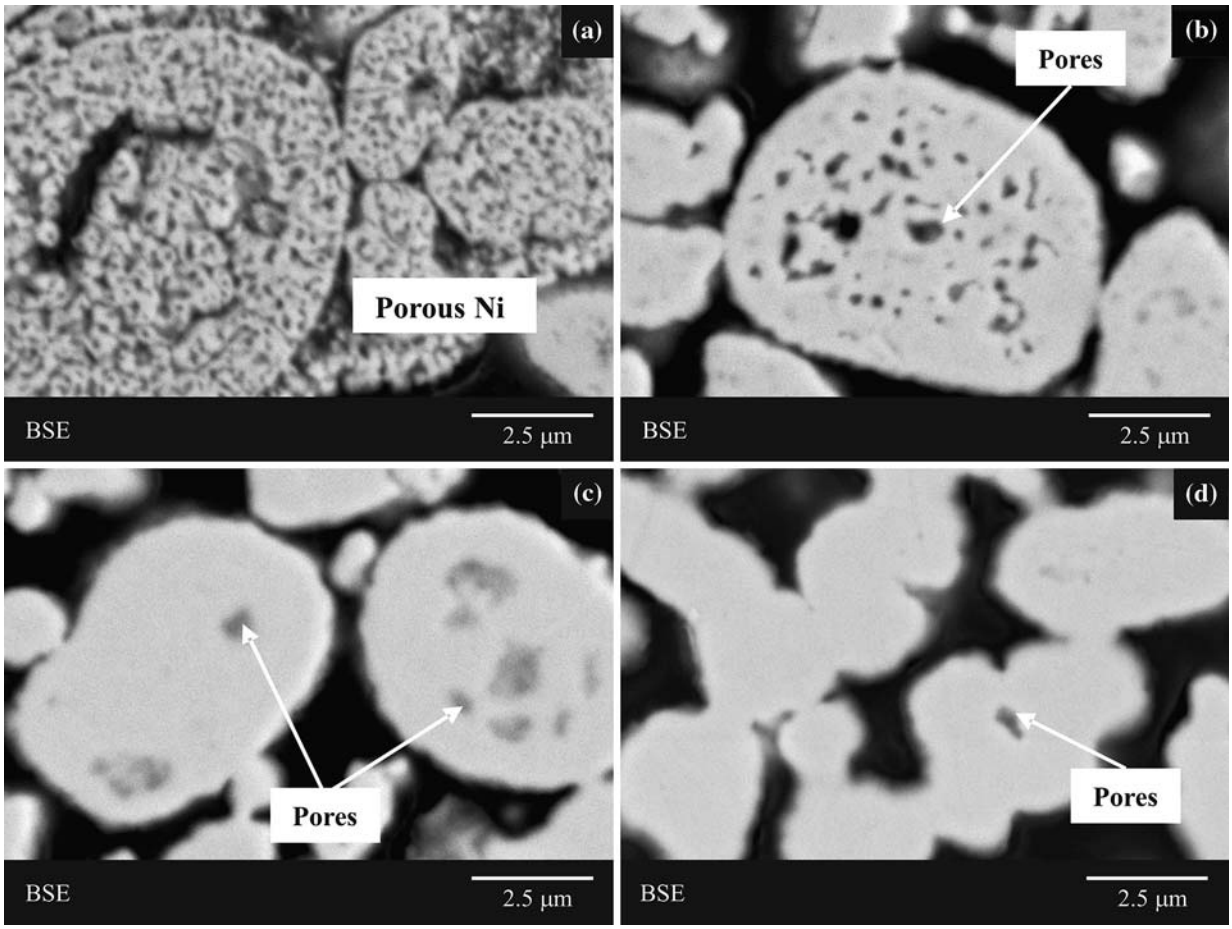

Fig. 14—SEM micrographs of the sections of the preoxidized (at 500 °C for 30 min) BNC sample reduced in 15 pct H_2-N_2 for 30 min at various temperatures: (*a*) 500 °C, (*b*) 700 °C, (*c*) 800 °C, and (*d*) 900 °C. The gray regions inside the particles are pores in the nickel product, not residual nickel oxide.

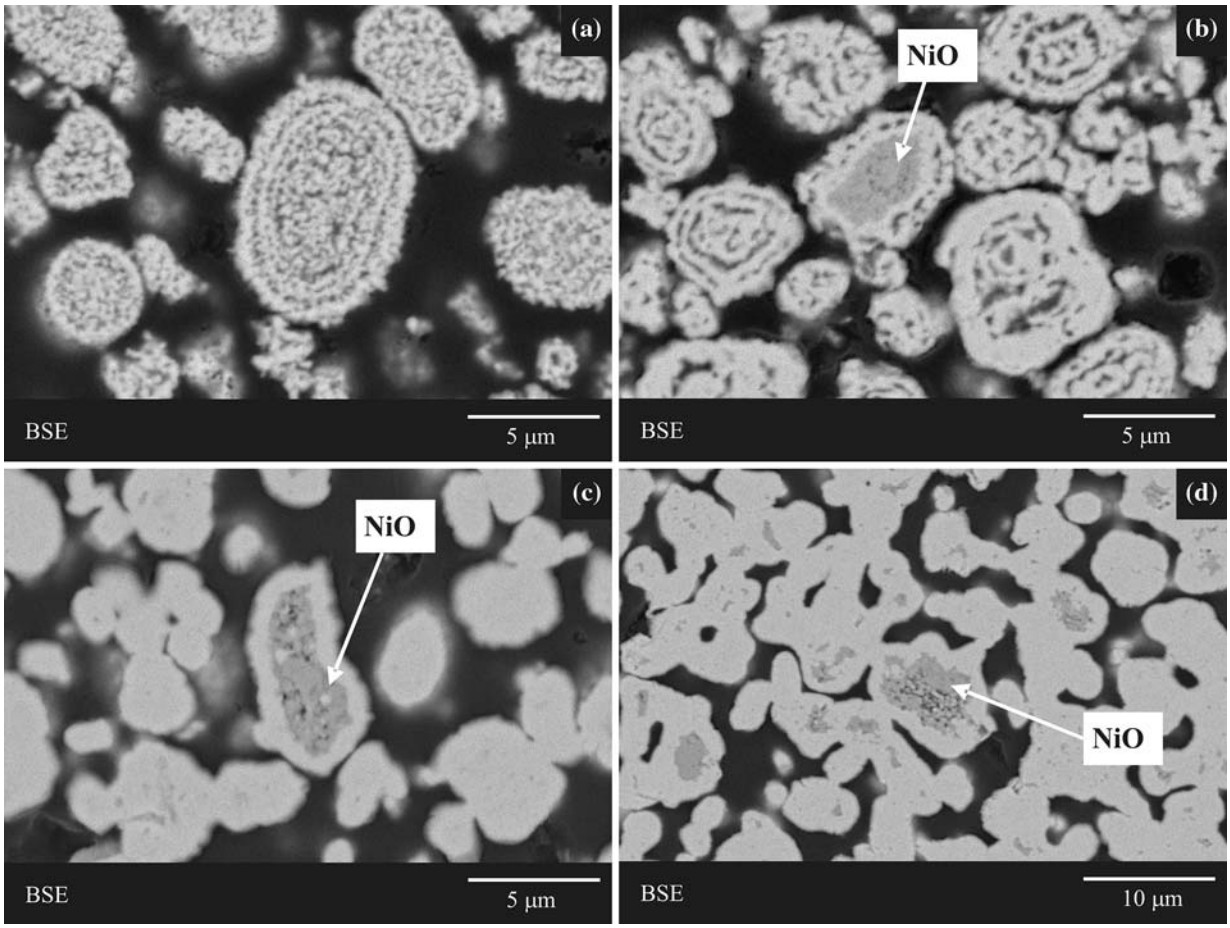

Fig. 15—Backscattered electron images showing internal microstructures of BNC reduced in 1.5 pct H_2-N_2; heating rate 10 °C/min at various temperatures: (*a*) 600 °C, (*b*) 700 °C, (*c*) 800 °C, and (*d*) 900 °C. The gray phases are the residual nickel oxide.

a significant effect on the microstructure evolution, and hence, on the final microstructure of the nickel product.

V. SUMMARY

A systematic investigation of changes in the phases present, the product surface, and the internal microstructures in basic nickel carbonate during controlled oxidation and reduction conditions at temperatures between 110 °C and 900 °C has been carried out. The results show that the thermal history and original microstructure of the material have significant effects on the microstructure evolution and, hence, on the final microstructure of the nickel product. The fundamental phenomena that are observed to contribute to the change of the physical and chemical characteristics of the particles during the process, affecting the final microstructure, are as follows:

1. chemical changes, *i.e.*, decomposition, reduction reactions, and oxidation reactions;
2. NiO and Ni recrystallization and grain growth; and
3. NiO and Ni sintering and densification.

The findings of the present study have clear implications for industrial practice, demonstrating that the key to achieving complete reduction of NiO by hydrogen gas is by controlling the relative rates of densification of nickel product and the overall reduction rate of nickel oxide. High extent of NiO reduction is favored by the following steps:

1. maintaining a high-NiO, specific surface area to avoid NiO and Ni recrystallization and densification, which is achieved by carrying out reduction below 600 °C; and
2. maintaining a high chemical rate, which is favored by high H_2 partial pressures and high H_2/H_2O ratios (*i.e.*, high chemical driving force for reduction).

ACKNOWLEDGMENTS

The authors thank the BHP Billiton Yabulu Refinery for supplying the basic nickel carbonate samples. The authors also acknowledge the financial support from the Australian Research Council and the BHP Billiton Yabulu Refinery as part of an ARC Linkage project. The authors further thank Mr. John Fittock and Dr. Joy Morgan (Yabulu Refinery) for valuable discussions. MAR also thanks Mr. Jiang Chen for carrying out the TGA/DTA measurements.

REFERENCES

1. H. Schmalzried: *Solid State Reactions*, transl. A.D. Pelton, Academic Press, New York, NY, 1974, pp. 166–70.
2. P. Delmon: in *Reactivity of Solids*, J.S. Anderson, ed., Chapman and Hall, London, 1972, pp. 567–75.
3. N.B. Hannay: *Treatise on Solid State Chemistry*, vol. 4, *Reactivity of Solids*, Plenum Press, New York, NY, 1976, pp. 193–280.
4. V.V. Boldyrev: *Reactivity of Solids: Past, Present, and Future*, IUPAC, Blackwell Science, Cambridge, United Kingdom, 1996.
5. J. Szekely, J.W. Evans, and H.Y. Sohn: *Gas-Solid Reactions*, Academic Press, New York, NY, 1976.
6. D.A. Young: *Decomposition of Solids, The International Encyclopaedia of Physical Chemistry and Chemical Physics, Topic 21, Vol. 1*, Pergamon Press, Oxford, United Kingdom, 1966, pp. 1, 38, 65, and 105.
7. J.H. Canterford: *Miner. Sci. Eng.*, 1975, vol. 7 (1), pp. 3–17.
8. L.L. Bergeson: EU's New Chemical Policy will hurt U.S. Competitiveness, *Chem. Process. Mag.*, Oct. 9, 2003, http://www.chemicalprocessing.com/articles/2003/143.html?page=print (accessed September 19, 2007).
9. *MSDS (Material Safety Data Sheet) Information*, http://www.hazsafety.pf.uq.edu.au/chemwatch/ (accessed September 19, 2007).
10. R.M. Mallya and A.R.V. Murthy: *J. Ind. Inst. Sci.*, 1961, vol. 43 (3), pp. 131–40 and 141–47.
11. W.M. Shaheen: *Mater. Lett.*, 2002, vol. 52, pp. 272–82.
12. H. Henmi, M. Mori, T. Hirayama, N. Mizutani, and M. Kato: *Thermochim. Acta*, 1986, vol. 104, pp. 101–09.
13. M. Hirai and H. Yamamoto: *J. Mass Spectrom. Soc. Jpn.*, 1998, vol. 46 (4), pp. 296–98.
14. S.A.A. Mansour: *Thermochim. Acta*, 1993, vol. 228, pp. 155–71.
15. F. Benton and P.H. Emmett: *J. Am. Ceram. Soc.*, 1924, vol. 46 (12), pp. 2728–37.
16. W. Pluschkell and B.V.C. Sarma: *Arch. Eisenhuttenwes.*, 1974, vol. 45 (1), pp. 23–31.
17. Y.K. Rao and A.H. Rashed: *Trans. Inst. Min. Metall, Sect. C*, 2001, vol. 110, pp. 1–6.
18. A.H. Rashed and Y.K. Rao: *Chem. Eng. Commun.*, 1996, vol. 156, pp. 1–30.
19. Y. Iida and K. Shimada: *Bull. Chem. Soc. Jpn.*, 1960, vol. 33 (9), pp. 1194–96.
20. T.A. Utigard, M. Wu, G. Plascencia, and T. Marin: *Chem. Eng. Sci.*, 2005, vol. 60, pp. 2061–68.
21. T.A. Utigard, G. Plascencia, T. Marin, A.E.M. Warner, J. Liu, A. Vahed, and M. Muinonen: *Can. Metall. Q.*, 2005, vol. 44 (3), pp. 421–28.
22. J.G. Reid and J.E. Fittock: *Proc. Int. Laterite Nickel Symp. 2004*, Mar. 2004, TMS, Warrendale, PA, pp. 599–618.
23. B.D. Cullity and S.R. Stock: *Elements of X-ray Diffraction*, Prentice-Hall International, Upper Saddle River, NJ, 2001, p. 170.